REPORT DOCUMENTATION PAGE

1a. REPORT SECURITY CLASSIFICATION UNCLASSIFIED	1b. RESTRICTIVE MARKINGS
2a. SECURITY CLASSIFICATION AUTHORITY	3. DISTRIBUTION / AVAILABILITY OF REPORT Approved for public release; distribution unlimited.
2b. DECLASSIFICATION / DOWNGRADING SCHEDULE	
4. PERFORMING ORGANIZATION REPORT NUMBER(S) NRL MEMORANDUM REPORT NO.	5. MONITORING ORGANIZATION REPORT NUMBER(S)
6a. NAME OF PERFORMING ORGANIZATION NAVAL RESEARCH LABORATORY Underwater Sound Reference Det 6b. OFFICE SYMBOL (If applicable) Code 5975	7a. NAME OF MONITORING ORGANIZATION
6c. ADDRESS (City, State, and ZIP Code) P.O. Box 568337 Orlando, Florida 32856-8337	7b. ADDRESS (City, State, and ZIP Code)
8a. NAME OF FUNDING / SPONSORING ORGANIZATION NAVAL RESEARCH LABORATORY 8b. OFFICE SYMBOL (If applicable)	9. PROCUREMENT INSTRUMENT IDENTIFICATION NUMBER
8c. ADDRESS (City, State, and ZIP Code) Washington, DC 20375-5000	10. SOURCE OF FUNDING NUMBERS PROGRAM ELEMENT NO. 61153N; PROJECT NO.; TASK NO. RR011-08-42; WORK UNIT ACCESSION NO. (59)-1472 DN280-003

11. TITLE (Include Security Classification)

Bulk Modulus of Elasticity of Various Elastomers: Theory and Experiment

12. PERSONAL AUTHOR(S)

Jay Burns*, Pieter S. Dubbelday, and Robert Y. Ting

13a. TYPE OF REPORT	13b. TIME COVERED	14. DATE OF REPORT (Year, Month, Day)	15. PAGE COUNT
Work in Progress	FROM Jul 84 TO Feb 87		38

16. SUPPLEMENTARY NOTATION

*Dr. Burns was employed under contract N62190-86-M-1169 with Jay Burns Scientific Consultants, N. Indiatlantic, FL 32903.

17. COSATI CODES		
FIELD	GROUP	SUB-GROUP
11	10	
20	11	

18. SUBJECT TERMS (Continue on reverse if necessary and identify by block number)

Bulk modulus
Elastomers
Free volume theory
Viscoelasticity

19. ABSTRACT (Continue on reverse if necessary and identify by block number)

A simple theoretical model for the bulk modulus of elastomers based upon the free volume concept is described. It gives a static (zero frequency) bulk modulus which exhibits a temperature dependence similar to chain theories of shear and Young's moduli. At higher temperatures, the model gives an Arrhenius-type behavior. The frequency dependence is developed from generalization of a single relaxation time hereditary model using the method Fuoss and Kirkwood applied to dielectric losses in polymers. The result yields simple hyperbolic functional dependencies of the storage and loss moduli upon frequency. These function are consistent with the time-temperature superposition principle and can be used to construc master curves using the WLF frequency shift method. Experimental data have been obtained for a number of rubbery elastomers using an acoustic coupler method. Details of the experimental arrangement are described together with results obtained. Generally, values of the bulk modulus are found to closely resemble those of typical organic liquids. Recent data have permitted construction of master curves for several samples, and the parameters for these curves are given.

20. DISTRIBUTION / AVAILABILITY OF ABSTRACT	21. ABSTRACT SECURITY CLASSIFICATION
☒ UNCLASSIFIED/UNLIMITED ☐ SAME AS RPT. ☐ DTIC USERS	UNCLASSIFIED
22a. NAME OF RESPONSIBLE INDIVIDUAL Pieter S. Dubbelday	22b. TELEPHONE (Include Area Code) (305) 857-5197 22c. OFFICE SYMBOL NRL-USRD Code 5975

DD FORM 1473, 84 MAR 83 APR edition may be used until exhausted.
All other editions are obsolete.

Naval Research Laboratory

Washington, DC 20375-5000 NRL Memorandum Report 5991 Date: June 5, 1987

Bulk Modulus of Elasticity of Various Elastomers: Theory and Experiment

Jay Burns

Jay Burns Scientific Consultants
N. Indiatlantic, Florida 32903

and

Pieter S. Dubbelday and Robert Y. Ting

Underwater Sound Reference Detachment
P.O. Box 568337
Orlando, Florida 32856-8337

CONTENTS

BULK MODULUS OF ELASTICITY OF VARIOUS ELASTOMERS: THEORY AND EXPERIMENT

INTRODUCTION

The mechanical characterization of linear homogeneous isotropic solids consists of the identification of two complex elastic moduli as functions of frequency, temperature, and pressure. In principle, any two moduli would be suitable since any pair of independent moduli may be converted into any other pair by relations well known from elasticity theory. The character of the experiments designed to measure a particular modulus differs considerably from one modulus to another, and the ones most easily measured are not necessarily the ones needed in a given application or relevant to the theory. Problems also arise with accuracy in converting between certain pairs of elastic moduli by the elastic theory relations mentioned above. For example, measurements of speed of sound in a bar is a favored method [1]. The corresponding elastic modulus so obtained is Young's modulus E. This value may be combined with a torsional or other determination of the shear modulus G [2,3]. If one wishes to obtain either the bulk modulus K or the plane-wave (dilatational) modulus M from E and G, a division by the factor (3G-E) is required. However, if Poisson's ratio is close to the value 0.5, as it is for most elastomers, the value of E is very close to 3G, and the divisor (3G-E) becomes very small. As a consequence, the slightest inaccuracies in either G or E are magnified greatly, and the resulting values of K or M have such large uncertainties as to mask any finer detail that might be of significance. For this and other reasons, it is desirable to have a direct measurement of the bulk modulus K, or the plane-wave modulus M [4].

One of these other reasons is that, from a theoretical standpoint, the bulk modulus arises from quite different mechanisms than the other elastic moduli. In particular, it is mostly a measure of the short-range inter- and intramolecular potentials and is little affected by longer range chain effects that dominate in shear and tension. Thus the theoretical information on molecular scale mechanics furnished by the bulk modulus is to an important degree complementary to that obtained from the other moduli. The bulk moduli of elastomers above their glass-transition temperatures are quite similar to those of organic liquids both in magnitude and in loss characteristics. This is consistent with the idea that short-range interactions dominate in determining the bulk moduli of both liquids and elastomers.

Implementation of a method to measure dynamic bulk moduli at the Underwater Sound Reference Detachment of the Naval Research Laboratory (NRL-USRD) was also based upon the desire to have an in-house experimental capability to assist in the development of new elastomers. Since the method to be described in this report may easily be extended to quite low audio frequencies, it can provide data on K in the frequency realm unattainable with the impedance tube and string methods. At the high-frequency end, the method provides some useful overlap with the latter methods so bulk, shear, and Young's moduli can be compared at the same frequency.

The bulk modulus is measured at NRL-USRD in an acoustic coupler similar to those used for reciprocity calibration of hydrophones. The method is very close to that of McKinney, Edelman, and Marvin [5]. The method will be described, the basic equations given, calibration and measurement techniques discussed, and preliminary results given for a number of different elastomers. In addition, results of a detailed analysis will be given for several elastomers to show the capability of the method to provide comparatively complete information about the bulk modulus of a material as a function of both temperature and frequency.

THEORY

Basic Free-Volume Model

Because of the close resemblance between the bulk moduli of elastomers and typical organic liquids, it appears likely that the free-volume theory of liquids can provide a suitable framework within which to understand the bulk moduli of the elastomers of interest in the present work.

In its basic form, the free-volume concept envisions a liquid above its glass-transition temperature as a somewhat spongy material consisting of many holes of molecular size imbedded in a highly compliant, loose structure. These holes vary widely in size but are distributed randomly throughout the material at any given instant. At or below the glass temperature T_g, the material is in the form of an amorphous, glassy solid. Such solids are quasi-crystalline in structure with the molecules almost, but not quite, arranged in the regular orderly manner of a crystalline solid. About each molecule in the glassy state there is a local volume over and above that actually occupied by the molecule itself. This local volume v_f is the "free volume." It forms "cages" on a molecular scale within which each molecule is constrained to move at low temperatures. There is little or no molecular transport possible below the glass-transition temperature.

At T_g a phase transition takes place, a sort of "melting" of the glassy state; this phase change is accompanied by a marked increase in the thermal expansion coefficient, α_T, of the material, by more than two orders of magnitude, as a rule. As the temperature rises further, the excess volume that accompanies the thermal expansion is distributed throughout the sample, but not uniformly. The excess free volume is, instead, randomly distributed among the N molecules of the sample, and some molecules therefore have relatively large holes around them, while others have only small holes as their share of the excess free volume. This process of redistribution of free volume is a continually changing one, but the time scale for such changes is estimated to be of the order of 10^{-12} second in typical liquids [6], long enough on the time scale of molecular motions for one to adopt a quasi-static picture of the structure within which, for the duration of its existence, one can calculate the distribution of free-volume hole sizes. Cohen and Turnbull [7] have given a derivation of the distribution function for hole sizes by considering the excess total free-volume V_f to consist of packets, one for each of the molecules in the sample with no restriction that the packets all be of the same size. A simpler derivation, restricted to packets of the same size, has been given by Bueche [8] (see also Appendix A). If all packets are

of the same size, it follows that the chance for a particular molecule, or molecular segment in the case of a polymer chain, to have $q=v_f'/v_f$ packets associated with it is

$$p(v_f') = (v_f/2\pi v_f')^{1/2} \exp(-av_f'/v_f) \ , \tag{1}$$

where $a=\ln q-1$. Turnbull and Cohen [9] and more recently Cohen and Grest [6] defined a critical value v_f^* for the excess free volume such that holes larger than v_f^* can contain molecules or molecular segments that are able to move about freely within the hole without encountering any energy barriers, much as a gas molecule might move within v_f^*. We adopt this two-phase, gas-phase model for the rubbery state of an elastomer above the glass temperature.

The elastomer is considered to contain holes of varying sizes, some of which are larger than v_f^* and may contain free-moving segments of molecules that behave like the molecules of a gas. The total pressure of such a gas phase in a sample at temperature T may be written as for an ideal gas:

$$P = N^*kT/V_f^* \tag{2}$$

where N^* is the total number of molecules (or segments) that are in the gas phase in holes larger than v_f^*. The total volume of these large holes is V_f^*.

We note that the isothermal bulk modulus K_T for an ideal gas is equal to its pressure, and the adiabatic modulus K_A is 5/3 the isothermal modulus. This relates Eq. (2) to the bulk modulus; our model is based on this equality. The model postulates that, as far as the bulk modulus is concerned, the elastomer behaves like an ideal gas contained in holes within a highly compliant matrix so the external pressure is transmitted freely throughout the solid, as it is in the case of a liquid. Corrections for the residual rigidity of the matrix can be made if necessary. They may be incorporated by considering the compliance of the elastomer to be the sum of the compliances of the gas and the matrix; i.e., the compliances are "in series."

V_f^* can be calculated from the hole size function, Eq. (1). The result is

$$V_f^* = A \exp\ (-aNv_f^*/V_f) \ , \tag{3}$$

where A and a are constants, N is the number of molecules in the sample, and V_f is the total sample volume. Note that $V_f=Nv_f$.

In order for a molecule to leave the "wall" of a hole and enter the gas phase, it must free itself from the forces that bind it to the wall, namely the attractive forces of its neighboring wall molecules. This evaporative process requires energy, and it follows that N must be proportional to a Boltzmann factor of form $\exp(-\epsilon/kT)$ where ϵ is the energy of vaporization. This energy is not a constant but depends upon the hole size for the same reason that the vapor pressure in a small bubble depends upon the size of the bubble. As the free volume vanishes at the glass-transition temperature, ϵ must also go to zero. In large holes that can exist at high temperatures, ϵ approaches a value comparable to the energy of vaporization of the material.

Putting these factors together into Eq. (2) gives, finally,

$$K = AT \exp(C/V_f - \epsilon/kT). \tag{4}$$

where $C=aNv_f^*$.

The total free-volume V_f in Eq. (4) is proportional to the total volume V of the sample and, therefore, it varies linearly with temperature and external pressure as

$$V_f = V_{fg} + \alpha_T V_g (T-T_g) - \beta_s P \tag{5}$$

where α_T is an appropriate volume thermal expansion coefficient, V_g is the total volume at T_g, and β_s is the compressibility of the solid. Since $\beta_s=K^{-1}$, inclusion of the $\beta_s P$ term makes Eq. (5) for K inherently nonlinear. However, at modest pressures, the $\beta_s P$ term is small and an average value of β_s may be used without appreciable error. This linearizes Eq. (5). In what follows, we take P 0 and omit the $\beta_s P$ term, treating only the temperature and frequency dependence of K. Extension to higher pressures is straightforward.

In Eq. (5), V_f is defined in such a way that it has the value V_{fg} at T_g, so the correct expansion coefficient to use in Eq. (5) is the difference between the expansion coefficients for the liquid phase and the extrapolation of the coefficient of the glassy phase. Figure 1 below shows more clearly the meaning of this statement.

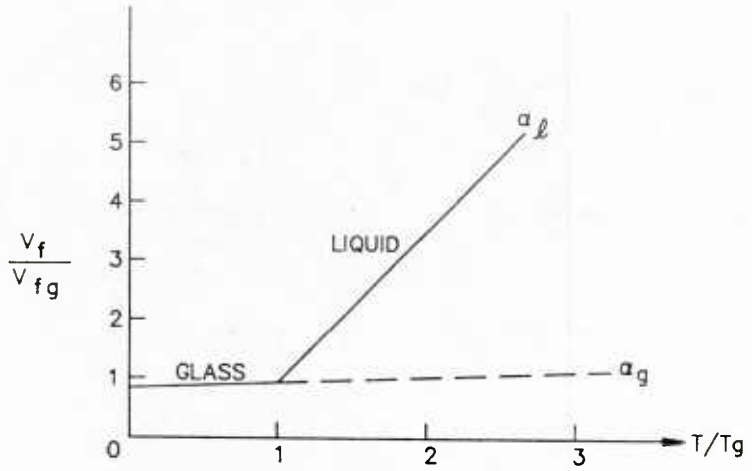

Fig. 1 - Thermal expansion coefficients of a typical elastomer in the vicinity of the glass-transition temperature.

The value of α_T to be used in Eq. (5) is $\alpha_T=\alpha_\ell-\alpha_g$, and the temperature variation of V_f is given by Eq. (5) with this value of α_T.

Substituting Eq. (5) into Eq. (4) and taking the logarithm of the resulting expression gives

$$\ell n(K/T) = A' - B/T + \frac{C}{V_f + \alpha_T V_g (T-T_g)} - \ln[V_{fg}+\alpha_T V_g(T-T_g)] , \qquad (6)$$

where $A'=N_s k/2$, $C=aNv_f^*$, V_{fg}, and α_T are all constants for a given material. N_s is the number of "surface" molecules or molecular segments lining all holes with $v_f>v_f^*$. The first term on the right is negligible compared with the third because $C/Nv_f \approx v_f^*/v_f \approx 40$, and $A'/N \approx N_s k/N << 0.025$. Also, the logarithmic term is small compared with the C/V_f term so Eq. (6) may be written more simply

$$\ln\ (K/T) = \frac{C}{V_{fg}+ \alpha_T V_g (T-T_g)} \qquad (7)$$

which is a good approximation not too far above the glass-transition temperature. It is often convenient for curve fitting to write this in the linear form

$$\left[\ln\ (K/T)\right]^{-1} = V_{fg} + \alpha_T V_g\ (T-T_g) = d + bT\ . \qquad (8)$$

WLF Frequency Shift Property of the Model

It is a simple matter to show that Eq. (7) leads to the Williams, Landel, Ferry [11] equation for the shift in frequency required to superimpose two values of K' or K" measured at different temperatures. This is the familiar WLF frequency shift method, though it will not appear here in its conventional form since we have not yet introduced the frequency dependence of K.

Consider two temperatures, T_1 and T_2. Write the free volume at T_2 as

$$V_{f2} = V_{f1} + \alpha_T V_1 \ (T_2 - T_1) \tag{9}$$

where V_1 is the total volume at T_1. Then, neglecting second order terms in α_T, Eq. (7) becomes

$$\ln(K_2 T_1 / K_1 T_2) = C(1/V_{f2} - 1/V_{f1}) = \frac{-c_1 (T_2 - T_1)}{c_2 + (T_2 - T_1)} , \tag{10}$$

where

$$c_1 = C/V_{f1} \quad \text{and} \quad c_2 = \alpha_T^{-1} \ V_{f1}/V_1 . \tag{11}$$

We note that the right-hand side of Eq. (10) has the form of the WLF equation for $\ln(a_T)$, the logarithmic frequency shift factor to make data taken at T_1 correspond with those taken at T_2 [12]. The constants c_1 and c_2 are identified with the material properties of the sample through Eq. (11). However, c_1 contains V_{f1} which depends upon the particular choice of reference temperature T_1. Bueche [10] has suggested that the product $c_1 c_2$=2080 for a large number of materials, and Ferry [13] has also shown that the product $c_1 c_2$ is a constant independent of the reference temperature. Our data do not support this universal value hypothesis; our values of c_1 and c_2 and their product vary appreciably from the "universal" values.

High-Temperature Behavior and the Arrhenius Factor

Before introducing dynamic factors we note that, at low temperatures below about 100 to 150°C above the glass temperature T_g, the ϵ/kT term is small compared with the other term, C/V_f, so the latter dominates at lower temperatures. However, at temperatures above about T_g+100°C, ϵ/kT becomes large enough to influence the modulus and, as found experimentally, this leads at higher temperatures to an "Arrhenius" type of behavior of K with temperature due to the $\exp(-\epsilon/kT)$ term. We shall disregard the Arrhenius term

in what follows. Nevertheless, the present model introduces this high-temperature behavior in a straightforward way and shows how the transition takes place between low- and high-temperature behavior.

Dynamical Considerations and Frequency Dependence

The frequency dependence of K may be introduced by way of relaxation theory which is fundamentally related to causality and is a necessary property of all macroscopic linear systems. Briefly, a linear system with a single relaxation time τ responds to an input F(t) to give an output of the form

$$H(t) = \int_{o}^{t} F(t') \exp[(t'-t)/\tau] \, dt' \ , \tag{12}$$

where F(t')=0 for all times t'<0. This simply means that the output at any time is the sum of all inputs at earlier times, each declining exponentially in amplitude with time. Applied to a sinusoidal input of circular frequency, ω, the result expressed in terms of the complex bulk modulus, K^*, takes the well-known form [14]

$$K^* = K' + iK'' \tag{13}$$

$$K' = K'_o + \Delta K \frac{(\omega\tau)^2}{1 + (\omega\tau)^2} \tag{14}$$

$$K'' = \Delta K \frac{\omega\tau}{1 + (\omega\tau)^2} \tag{15}$$

where K'_o is the limiting value of K' as frequency goes to zero, and $\Delta K = K'_\infty - K'_o$ where K'_∞ is the limiting value at high frequency.

In the equations above, the complex bulk modulus K^* is the combination of an in-phase "storage modulus," K', and an out-of-phase "loss modulus," K".

Define a logarithmic frequency scale by

$$x = \ln(f/f_m) \text{ where } f_m = 1/2\pi\tau \text{ and } f = \omega/2\pi \ . \tag{16}$$

Then Eqs. (14) and (15) can be written in the form

$$K' = K'_o + \frac{\Delta K}{2} (1+\tanh x) \tag{17}$$

$$K'' = \frac{\Delta K}{2} \text{ sech } x \ . \tag{18}$$

In their study of dielectric losses in polymers, Fuoss and Kirkwood [15] showed that the imaginary part of the dielectric constant that has the same form as Eq. (18) could be generalized to the case of a continuous distribution of relaxation times by simply introducing a "spread factor," α, that multiplies x in Eq. (18). (α is positive, real, and ≤ 1.) They also showed that the spread factor determines a relaxation time spectrum of the polymer. We adopt this generalization for the bulk modulus and write

$$K' = K'_o + \frac{\Delta K}{2} [1+\tanh (\alpha x)] \tag{19}$$

$$K'' = \frac{\Delta K}{2} \text{ sech } (\alpha x) \ . \tag{20}$$

Appendix B gives an abbreviated form of the Fuoss and Kirkwood generalization and their expression for the relaxation time spectrum, $G(\tau)$, which depends upon α.

If the principle underlying the WLF shift method is to hold, it is necessary that curves of K' and K" vs frequency measured at different temperatures be similar in shape so they can be superimposed by suitable shifting along the frequency scale, the amount of such shift being determined by the difference in temperature of a given curve relative to a chosen reference temperature. It is therefore required that $K'(T_1)=K''(T_o)$ under a frequency shift from $x(T_1)$ to $x(T_o)$ where

$$x(T_o) = x(T_1) - (x_{i1} - x_{io}) \ . \tag{21}$$

The subscript "o" identifies a reference temperature which may be chosen arbitrarily and the subscript i identifies the inflection point of the $K'(x)$ curve or the maximum of the $K''(x)$ curve.

Figure 2 shows the rationale for Eq. (21).

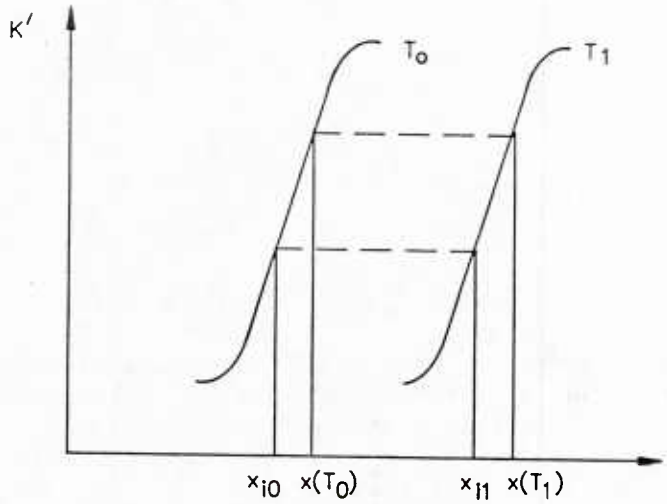

Fig. 2 - Curves of K'(x) at two temperatures; x is a logarithmic frequency defined by Eq. (16).

It is clear from Fig. 2 that a log frequency shift of the amount $(x_{i1}-x_{io})$ is needed to superimpose the T_1 curve upon the T_o one. Thus, any point x on the T_1 becomes a corresponding point on the T_o curve under the shift $(x_{i1}-x_{io})$, and Eq. (21) expresses this. Since $x=\ln(f/f_m)$, Eq. (21) may be written

$$x(T_o) = x(T_1) - (x_{i1}-x_{io}), \text{ or } \ln[f(T_o)/f(T_1)] = \ln[f_m(T_o)/f_m(T_1)]. \quad (22)$$

Thus,

$$f(T_o)/f_m(T_o) = f(T_1)/f_m(T_1). \quad (23)$$

It follows that $(x-x_m)$ is invariant with respect to changes in temperature, and this is the proper variable to use in the argument of the hyperbolic functions in K' and K". Therefore, Eqs. (19) and (20) should be written

$$K' = K'_o + \frac{\Delta K}{2}\{1+\tanh[\alpha(x-x_m)]\} \quad (24)$$

$$K'' = \frac{\Delta K}{2}\,\mathrm{sech}\,[\alpha(x-x_m)] \quad (25)$$

with

$$x_m(T) - x_m(T_o) = \frac{c_1^o(T-T_o)}{c_2^o + (T-T_o)} \tag{26}$$

where c_j^o is the value of c_j at reference temperature T_o.

The frequency dependence of the model is contained in Eqs. (24) and (25) which, as we have shown, also exhibit the WLF shift property. At present, we are uncertain how these equations should be combined with the zero frequency expression Eq. (4) to produce a complete description of both frequency and temperature dependence in a single expression. A simple approach would be to argue that since the loss modulus K" is proportional to the viscosity, the ΔK factor that multiplies $\mathrm{sech}(x-x_m)$ should have the form of Eq. (4).

The losses depend upon the viscous forces acting in the medium, whether solid or liquid. In fact, the lossy part of the Young's and shear moduli are proportional to the coefficient of shear viscosity, η [16,17]. It is reasonable to assume the existence of a compressional viscosity which determines the loss bulk modulus K" in the same way, although the loss mechanisms will not be the same. In the shear case, the viscosities of many organic liquids obey a relation of the form

$$\eta'(T) = \eta'(T_o)\frac{T}{T_o} \exp\left[C/V_f(T) - C/V_f(T_o)\right]. \tag{27}$$

This was determined empirically by Doolittle [18] and is commonly referred to as the Doolittle equation. In Eq. (27) it has been cast in the form suggested by the free-volume theory of liquids [19], and η is proportional to one of the factors in Eq. (4). Thus we already have a viscosity term in the expression for K^* at very low frequency. Since K" must be proportional to the viscosity, it follows that K" in Eq. (25) must be modified to incorporate the viscosity term. This modification is guided by the condition that, as frequency goes to zero, the bulk modulus must reduce to the form of Eq. (4). The final result is that ΔK is proportional to the right-hand side of Eq. (4) which makes ΔK a function of T instead of a constant, as it is in Eqs. (24) and (25). This, in turn, destroys the frequency shift property because the frequency shift in this case does more than simply move the K' and K" curves along the frequency axis unaltered in shape; a frequency shift is also accompanied by a change of shape through the temperature dependence of ΔK.

For the present, we will treat the frequency dependence as given by Eqs. (24) and (25) in an ad hoc manner, considering Eq. (4) to be the fundamental result of the free-volume approach via our model. We therefore take ΔK to be a constant for a given sample and use the WLF method to construct master curves of K' and K" as functions of frequency at a reference temperature T_o. This process determines the parameters c_1 and c_2 of the WLF shift factor a_T where, by definition, $\log a_T = -(x-x_m)$, or

$$\ln(a_T) = -(x-x_m) = \frac{-c_1 (T-T_o)}{c_2 + (T-T_o)} \quad . \tag{28}$$

In addition to these parameters, the spread factor α, and the parameters K'_o and ΔK are found by fitting the curve obtained by the WLF method to the forms of Eqs. (24) and (25). This completes the parametric description of the master curves.

There are six parameters in all, and fitting in the general case proves to be difficult. Fortunately, in many cases, some of these parameters can be determined by methods other than a brute force computer approach. For example, if the data at the reference temperature T_o include the inflection point of K', the value of f_m can be found by inspection. Differentiation of Eq. (24) with respect to x gives

$$dK'/dx = \alpha\frac{\Delta K}{2} \operatorname{sech}^2 [\alpha(x-x_m)] \quad . \tag{29}$$

Fitting the experimental values of the slopes to a hyperbolic secant-squared curve of the form of Eq. (29) also determines the parameters α, ΔK, and the WLF parameters c_1 and c_2. (See Appendix C)

Ferry [19] has shown that the product $c_1 c_2$ should be a constant independent of temperature. This means that only one of these c's is an independent parameter. If this is correct, only three parameters would be needed to fit the slopes to Eq. (29), and the fitting process would be considerably simplified. Our data generally do not support the claim that $c_1 c_2$ is a constant for different samples, however, and this is puzzling since it runs counter to predictions of the WLF theory. Ferry himself [19] gives experimental data on shear moduli together with values of c_1 and c_2 which do not fully satisfy the constant product requirement of theory.

McKinney and Belcher [20] and Bueche [21], among others, have suggested that the fractional free volume at the glass-transition temperature is very nearly the same for all glass-forming liquids and may be considered to be approximately a "universal" constant whose value is 0.025. Bueche [21] has derived an expression for the thermal expansion coefficient of a liquid based on the free-volume concept. This theory supports the idea that the expansion coefficient is approximately $4.8\times10^{-4}\,(°C)^{-1}$ for most liquids in the temperature range up to about 100°C above T_g. With these values of free volume and expansion coefficient, the WLF a_T factor may be written in "universal" form

$$\ln(a_T) = \frac{-40\ (T-T_g)}{52 + (T-T_g)} \quad . \tag{30}$$

This is the form suggested by Bueche. Parenthetically, it implies that $v_f^* \approx 40v_{fg}$; that is, a hole about 40 times larger than the average size of a hole at T_g is needed to accommodate a molecular segment. Thus, many "average" holes must aggregate in order to form a hole of sufficient size into which a segment can jump in the liquid or rubbery state. Bueche's argument shows that c_1 and c_2 are related to physical constants of a given liquid and by inference to the corresponding constants of a given elastomer. Unless these constants vary more widely in elastomers than in liquids, which is certainly possible, and, unless they are much less interrelated in elastomers than in liquids, it is surprising that we do not find their product to be more nearly constant in the materials we have studied. As mentioned above, the data Ferry gives [19] on a variety of different elastomers also fail to support the constancy of the product $c_1 c_2$. No reason for this has been suggested.

Relaxation Spectrum

From a theoretical point of view, one of the more interesting kinds of information one would like to get from elastic modulus measurements on elastomers is the relaxation-time spectrum associated with the loss mechanisms in the materials.

Fuoss and Kirkwood [15] have shown that the spread factor determines a relaxation spectrum given by

$$G(\tau) = \frac{\alpha\tau_m}{\pi\tau}\left[\frac{\cos(\alpha\pi/2)\ \cosh(\alpha s)}{\cos^2(\alpha\pi/2) + \sinh^2(\alpha s)}\right] \tag{31}$$

where s is defined as $-\ln(\tau/\tau_m)$. (See Appendix B for details.)

It should be pointed out that only two parameters are required to completely determine the relaxation spectrum: the spread factor and the time-scale factor τ_m or its equivalent $f_m(=\tau_m^{-1})$, the frequency at the inflection point of K or at the maximum of K . The spectrum $G(\tau)$ is a $1/\tau$ spectrum modified by the factor in brackets in Eq. (31). When plotted against the logarithm of τ, Eq. (31) has the form shown in Fig. 3 below. The result clearly depends on the assigned value for the spread factor α.

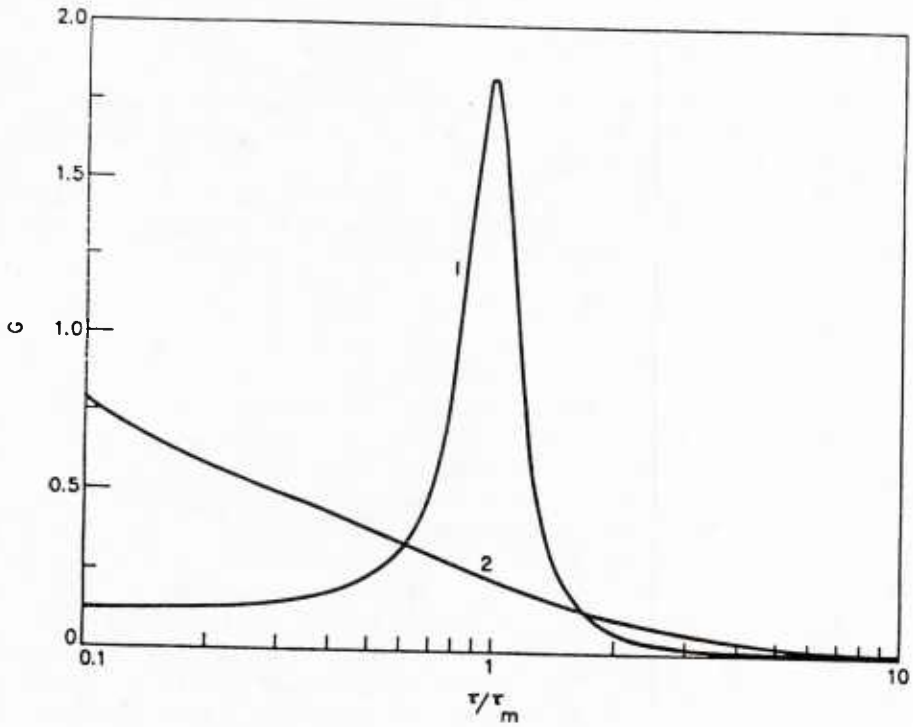

Fig. 3 - Form of the relaxation spectrum $G(\tau)$
(1) α=0.9 and (2) α=0.5.

In general, this type of spectrum is typical of liquid behavior. The experimental value of f_m falls in the range 0.1 to 1 kHz for several elastomer samples measured at NRL-USRD so τ_m is about 1 millisecond, and the spectrum typically extends to relaxation times well below 0.1 μsec with short relaxation times of the order of 1 μsec or less predominating. The $1/\tau$ character of relaxation spectra exhibited experimentally by our elastomer samples are typical of liquids and are consistent with free-volume theories for normal liquids (Cohen and Grest [6]). By contrast, various chain theories [22] of tensile and shear moduli predict more or less $\tau^{-1/2}$ relaxation spectra [23]. The difference in τ-dependence between shear and bulk (liquid) theories is pronounced and is an indicator of the difference in molecular mechanisms that operate in bulk as compared with shear or tension. In liquids, short-range interactions are dominant in determining compressive properties, while in shear it is primarily longer range chain entanglements and interactions that give rise to energy transfers that account for relaxation processes.

It should be pointed out that the shape of the relaxation spectra given by Fuoss and Kirkwood is a prediction of their theory and has not been verified experimentally. Therefore, it may or may not reflect the true relaxation spectrum of a real elastomer. Until there is experimental support for the spectra predicted by this theory one must exercise some care in relying upon such spectra to yield information about molecular processes.

If more than one relaxation mechanism operates in a material one would expect to find a superposition of K' and K'' curves, each with a set of parameters: α, ΔK, K'_o, and f_m. There would also be a superposition of

relaxation spectra $G(\tau)$ centered on different τ_m and each with a different α. Such superpositions can make the experimental K' and K" curves appear quite different from the simple form we have dealt with so far, particularly if the spectra of the different relaxation processes are not widely separated in frequency. We note this generalization but will not deal with it further in this report. We have not seen clear evidence for more complex K' curves in the limited experimental data obtained to date.

EXPERIMENTAL

There are two principal ways in which the dynamic bulk modulus of a solid material can be found experimentally. One is the impedance tube method in which the speed of transmission of a plane wave through a plane sample is measured. From this, the plane-wave modulus M is found, and the bulk modulus K can be calculated from the fundamental relation K=M-4G/3, provided the shear modulus G is also known. As mentioned earlier, in the materials of interest in the present work G is at least two orders of magnitude smaller than M, so K equals M to within 1% or better. There are technical difficulties in making accurate measurements by the impedance tube method, mostly connected with edge effects when the sound wavelength is not negligibly small compared with the dimensions of the sample. However, useful results can be obtained with this method with due care. It is especially useful at frequencies in the kHz range and complements the acoustic coupler method which is best at lower frequencies.

The second method is the acoustic coupler method developed in 1955 at the National Bureau of Standards by McKinney, Edelman, and Marvin [5]. The method employs a heavy-wall, steel pressure vessel in which there is a cavity containing two piezoelectric transducers, in addition to the sample and a filling fluid whose compressibility is accurately known as a function of both temperature and pressure. One of the transducers, the "driver," acts as a volume expander and, as its volume changes in response to an applied voltage, a pressure change is produced in the chamber. The pressure acts on the receiver transducer to produce an output voltage that is a measure of the resulting pressure change in the chamber. Therefore, the ratio of output to input transducer voltages carries information about the compliance of the coupler contents and particularly about the compliance of the sample.

The coupler used at NRL-USRD for the calibration of hydrophones has been described by Bobber [24]. For the present application the same kind of heavy steel chamber is used except that only two of the customary three ports are needed, one for a driver transducer and one for a receiver. Reciprocity is not required of the transducers in the present case. To make this point clear and to show the approximations made in the basic equations, the main line of the derivation is given here. It follows closely the analysis of McKinney, Edelman, and Marvin.

The sum of the changes of volume ΔV_i of all the items inside the coupler equals the change of volume of the cavity, ΔV_c, or

$$\Delta V_c = \sum_i \Delta V_i \ . \tag{32}$$

It is essential to assume that the pressure changes ΔP throughout the cavity are uniform; i.e., ΔP must be the same everywhere in the cavity during the pressure cycle produced by the driver which acts as a volume expander. This sets an upper limit to the frequency that may be employed in a given chamber. Dividing Eq. (32) by ΔP,

$$\frac{\Delta V_c}{\Delta P} = \sum_i \frac{\Delta V_i}{\Delta P} \ . \tag{33}$$

For the passive material; i.e., everything in the chamber including the chamber itself but excluding the transducers, one may set

$$-\frac{1}{V}\frac{\Delta V}{\Delta P} \approx -\frac{1}{V}\frac{dV}{dP} \equiv \beta = K^{-1} \ , \tag{34}$$

where K is the bulk modulus and β is the compressibility. For active materials, specifically the piezoelectric transducers in the chamber, one may write in the linear region,

$$E = aP + bu$$

and

$$I = cP + du \tag{35}$$

where E is the voltage across the transducer, I is the current through the transducer, u is the volume velocity, P is the pressure in the cavity, and a, b, c, and d are properties of the transducer material. These relations are applied to the driver and receiver in the coupler, indicated by indices 1 and 2, respectively. It is not necessary to assume reciprocity of either transducer. By algebraic manipulation, the electrical parameters of the two transducers may be related to the respective material parameters of the driver and receiver. For instance, the ratio of driver to receiver voltages is given for the open receiver circuit case by

$$R = \frac{E_1}{E_2} = \frac{b_1 d_2 \left[i\omega C - \frac{c_2}{d_2} - \frac{a_1}{b_1} \right]}{b_2 c_2 - a_2 d_2} \tag{36}$$

where C is the total compliance of all the passive materials in the coupler minus the chamber compliance.

To calibrate the chamber, one measures the above voltage ratio R_o when the chamber is filled with a fluid of known compressibility β_o, and again when the coupler contains a metal of known volume V_b and known (small) compressibility β_b. In this case, the voltage ratio is R_b. Measuring the voltage ratio R_s with an elastomer sample of volume V_s in the coupler, the compressibility β_s of the sample may be calculated from the following expression which is easily derived from Eq. (36). It gives the sample compressibility in terms of measured voltage ratios for the coupler containing, variously: brass, the unknown sample, and only oil. The relation is

$$\frac{\beta_s-\beta_o}{\beta_o} = \frac{-V_b}{V_s}\left(1-\frac{\beta_b}{\beta_o}\right)\frac{R_o - R_s}{R_o - R_b} . \qquad (37)$$

All of the R ratios in this expression are complex numbers, as Eq. (36) suggests. In general, β_s will be a complex number whose real part gives the storage compressibility of the sample and whose imaginary part gives the loss compliance. Both β_o and β_b are, for all practical purposes, real because the fluids used in these measurements and the metal calibration materials (brass in the present case) have very low losses, well below the limit of detection of our apparatus, which is to say below about 0.002 in loss tangent.

Figure 4 shows schematically the principle of the coupler and the electrical arrangement used.

A second coupler has been built with simple cylindrical geometry having a somewhat longer cavity, but otherwise similar to the first one. Both chambers accommodate cylindrical samples of 38-mm diam and 38-mm length. Castor oil has been the fluid used in our work to date, and accurate values for its static compressibility are known [25] over a wide range of temperature and pressure. Some preliminary work has been done using di-2 ethyl hexyl sebacate, a plasticizer used by McKinney and his coworkers at the National Bureau of Standards. This material is, unfortunately, reactive with a number of materials of interest in our work and, while its compressibility is accurately known, and while it has the advantage over castor oil of having a much lower viscosity allowing it to be used at much lower temperatures, its reactivity has ruled out its further use in our work

The "working" equation for the coupler has been given in Eq. (37) which relates the compressibilities β_s, β_b, and β_o of the sample, brass standard, and oil, respectively, to the measured voltage ratios R_s, R_b, and R_o. This equation is based upon a calibration of the system by substitution in which measurements of voltage ratios are made at each temperature and pressure of interest as functions of frequency under three conditions: oil in the

coupler, oil plus a brass sample comparable in size to the elastomer sample, and, finally, oil plus the elastomer sample itself. Since the brass sample is virtually incompressible in comparison with the oil, this calibration procedure actually compares the compliance of the oil displaced by the brass with the compliance of the elastomer sample. A small correction is made for the compliance of the brass, but typically this correction is of the order of 1%.

The choice of suitable transducers is crucial for good accuracy and high precision in the measurements. Long-term transducer stability is important for maintenance of calibration. It is also important that the transducers come rapidly to thermal and electrical equilibrium after changes in temperature or pressure. After some not very satisfactory experience with other transducers, we arrived at a suitable design using stacks of samarium-modified lead titanate disks 0.75 cm by 0.063-cm thick, four disks to a stack. The disks are made by the Edo Western Corporation with silvered faces for electrical contact. Thin metal foils are placed between the disks to provide external electrical leads and the stack is cemented together with epoxy. The stack is mounted, again with epoxy, to electrical feedthroughs and surrounded by an electrically grounded mesh screen for protection against accidental contact with the sample. The disks in each stack are electrically connected in parallel giving a total capacitance of about 1300 pF. The stack resonance frequency is quite high, about 145 kHz. By comparison, the acoustical resonance of the coupler used for the measurements reported here falls at about 8.3 kHz with no sample in the chamber. Thus the electrical resonance is high enough not to affect the measurements.

Figure 4 shows the early electrical setup for the system. In this arrangement, a Wavetek Model 185 sweep-frequency generator delivered a constant sinusoidal voltage of slowly increasing frequency to the driver transducer. The output voltage from the receiver transducer was fed into a PAR 5204 lock-in analyzer synchronized with the Wavetek frequency. The PAR output was then fed into a HP 7015B X-Y recorder whose X axis was driven by a signal voltage from the Wavetek that was proportional to the frequency of the signal generator. In this way, plots were created of the receiver transducer output voltage vs frequency. The driver input voltage was held constant so the plots could be converted into voltage ratios R for use in Eq. (37). The PAR also gives quadrature components of the input signal that were recorded in such a way as to give phase shifts as functions of frequency. These phase shifts were used to determine the lossy part K'' of the bulk modulus whereas the in-phase voltage ratios determined the storage modulus K'.

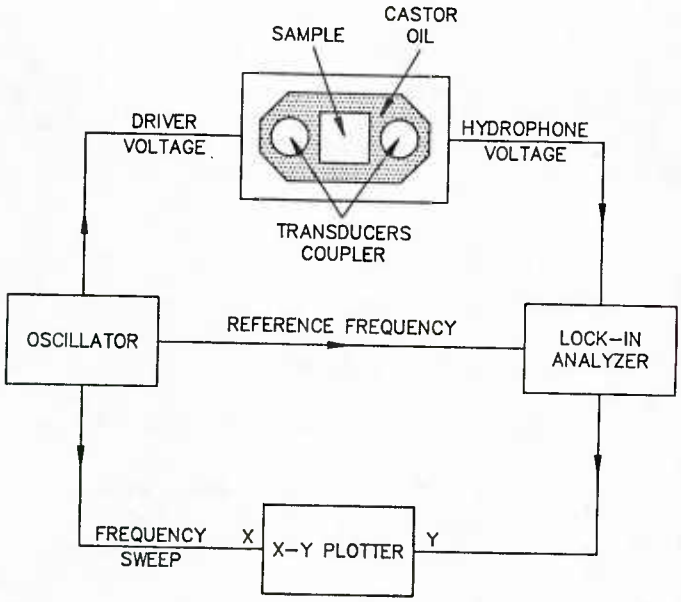

Fig. 4 - Electrical arrangement.

Accuracy and repeatability achieved with the analog measurement system described above was, at best, fair. Eventually we were able to reduce the uncertainty in K' to about ±8% and in K" to about ±30%. With this level of uncertainty it was only possible to determine major features of the bulk modulus, but finer details and, most important, the shift factors could not be found with sufficient accuracy to construct good master curves. Therefore, the system was converted to a largely digital measuring setup under computer control.

The improved system uses a Rockland Model 5100 frequency synthesizer which is programmed to produce a sequence of fixed frequencies at logarithmically spaced intervals. Control is provided by an Apple IIe computer working through a Rockland Interface Model 1488A using standard IEEE 488 bus protocol. The Rockland synthesizer produces a superior waveform with virtually unmeasurable distortion or frequency modulation. Its voltage output is also much more stable in amplitude than that of the Wavetek.

The receiver transducer output is still fed into a PAR 5204 lock-in analyzer as before, but now all signals both into and out of the coupler go through a HP 59307A VHF switch. This is a very low-noise, solid-state switch under computer control which allows measurements to be made of input and output voltages in programmed sequence. The switch also controls the outputs of the Keithley 195A digital voltmeters that read the PAR in-phase and quadrature outputs. The DVM's are under computer control as well, as they read the PAR outputs for both the driver and receiver transducer voltages and save the digitized voltages to a disk data file.

Several additional improvements were made. Better electrical shielding was employed, notably in regard to grounding. Acoustical noise isolation was provided between the coupler and the constant temperature bath that thermostats the coupler. The use of a much better bath permitted temperature control to a fraction of a degree. Finally, all computations are now made

from the raw data and calibration files stored on disk, reducing chances of computational error and providing for flexibility in whatever type of smoothing or data manipulation might be desired. The data files are interfaced to the NRL-USRD VAX computer which provides parametric curve fitting routines to fit experimental K' and K" values to the theoretical master curves. The net reduction in uncertainty in the K' and K" results has been impressive. It is now routine to obtain uncertainties in K limited by uncertainties in the reported compressibility of castor oil (about ±2%). Otherwise, the uncertainties in K' would be under ±1%. As for K", the uncertainties in direct measurement are much better than before, now having been reduced to about ±8%. However, by determining K" from K', as discussed earlier, it is possible to obtain K" to approximately the same accuracy as K', namely about ±1%. At these levels of uncertainty the WLF shifts can be determined with good accuracy for most samples and, from these, the master curves can be generated. The latter provide the full range of information about the bulk modulus and are the goal of most elastic modulus measurement programs.

RESULTS

Results of our measurements to date fall into two categories: (1) low-precision results on a relative wide variety of rubbery elastomers, and (2) high-precision results on several elastomer samples from which master curves and relaxation spectra have been obtained.

The "low-precision" results were obtained with the early analog, manually controlled version of the equipment. The uncertainty in K" values was too large to permit more than rough qualitative conclusions about the relative magnitude of K' and K" where it was found that the loss tangent ($\tan\delta$=K"/K') was small for all the elastomers tested. Small in this case means less than about 0.05 over the range of variables employed, and usually $\tan\delta$ was appreciably less than 0.05. The later high-precision measurements confirmed these findings quantitatively and, in fact, showed that the neoprene samples had loss tangents around 0.02 or less.

The first group of results is shown in abbreviated form in Fig. 5. The vertical bars of the figure represent ranges of measured values of K' at 10°C over the frequency span from 0.1 to 3 kHz. K' depends linearly upon frequency in this range. Among the 13 different kinds of elastomers shown in this figure are 3 natural rubbers, 4 neoprenes, 2 polyurethanes, and 1 representative sample each of polybutadiene, chloroprene (HT1066), butyl, and nitrile rubbers.

A significant point to note in Fig. 5 is that K' for all samples varies relatively little over the range of temperatures and frequencies employed. In fact, K' falls within ±35% of the mean value of 2.9 GPa, a value typical of organic liquids. One can see that the neoprenes have generally slightly higher than average bulk moduli while polyurethanes and natural rubbers are somewhat softer. The various other samples fall close to the average. Castor oil, the fill fluid which is a typical organic liquid falls at about 2.5 GPa, or a little less than the average for the elastomers tested. Another feature of these measurements is the fact that the loss tangents are small over the ranges of temperature examined. While the accuracy of the loss moduli was not good, it was sufficient to show that loss tangents were generally below 0.1.

Subsequent high-precision measurements confirmed that, indeed, they were less than 0.05 and, ordinarily, less than 0.02, again rather like liquids.

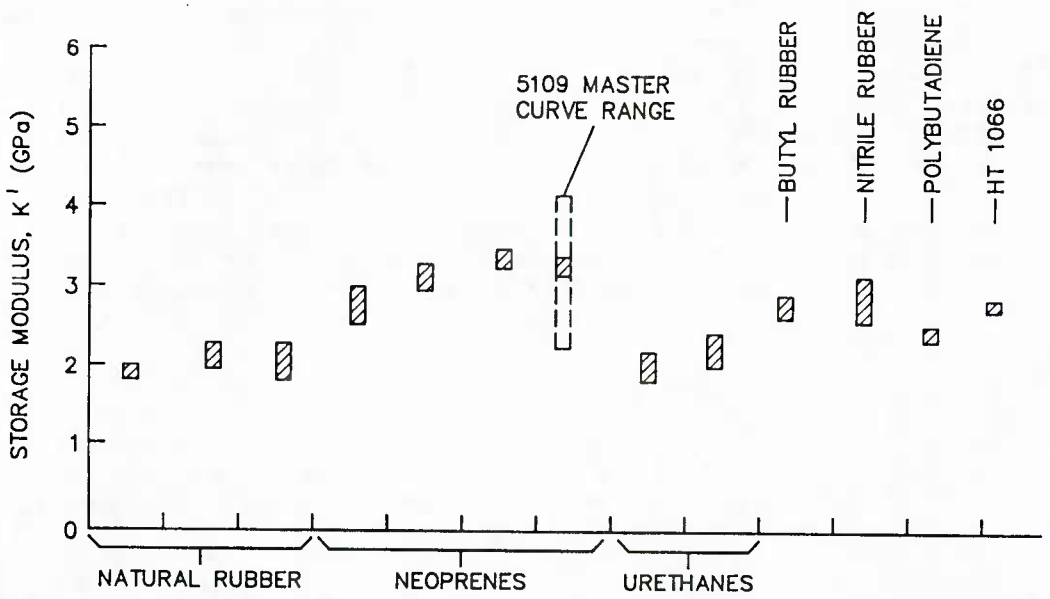

Fig. 5 - Storage modulus K' for various types of elastomers. (Bars give ranges of K' values at 10°C for frequencies 100 to 3000 Hz.)

As regards pressure dependence of the bulk modulus, some early measurements were made at pressures as high as 20 MPa, and K' was observed to increase with pressure, as it should. The increase was scarcely evident at pressures below 5 MPa, however, and since interest in the bulk moduli of the 13 samples measured initially lay in the low-pressure range 0 to 5 MPa, the results reported here were all at 2.5 MPa. It may be pointed out that the general formulation of the theory embodied in Eqs. (4) and (5) contains the effects of pressure implicitly in the volume term V_f as expressed in Eq. (5). We plan to explore the pressure dependence in later experimental work when a form of Eq. (7) that depends explicitly upon pressure as well as upon temperature will be used.

Figure 6 shows the master curves for a typical neoprene sample (5109). The reference temperature in this plot is 27°C which is the value of T_m at a frequency of 190 Hz as determined from a parametric fix of the experimental data. The parameters determined by the fitting process are given in the figure (K" is plotted from the parameters obtained from the K' data). The experimental points on the K' plot are those measured at 100 Hz over a range of T from -10°C to +40°C at a pressure of 2.5 GPa. Other points measured at different frequencies from 50 to 1500 Hz have been omitted for clarity, but they also fall quite close to the theoretical line shown. Results in Fig. 6 are typical of the high-precision, digital measurements made to date.

We note here, parenthetically, that we have found a more convenient way to find the WLF shift parameters than the one commonly used. This method is treated in Appendix C.

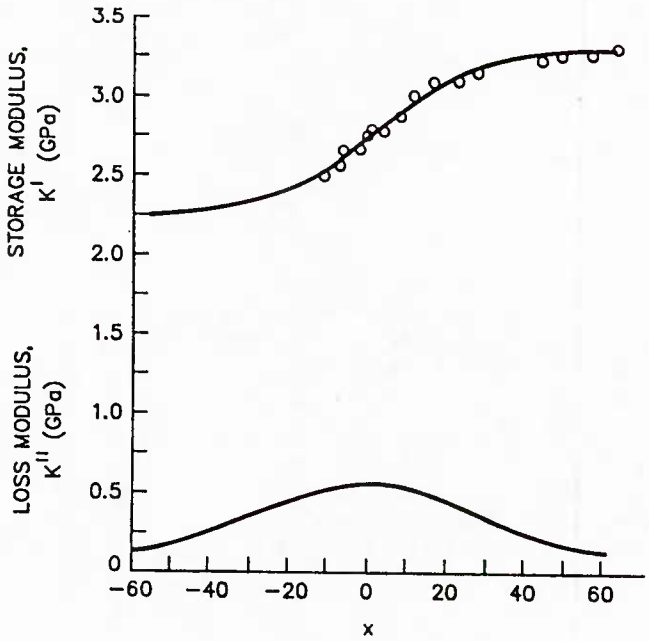

Fig. 6 - Master curves of K' and K" as functions of logarithmic frequency for Type 5109 neoprene. Parameters for these curves are α=0.037, K'_o=2.37 GPa, ΔK=1.1 GPa, f_m=190 Hz, and T_m=27°C. K" is computed from the K' data fit.

Since experiment and theory agree well, it is convenient to characterize the bulk moduli by the parameters K'_o, ΔK, and α. From these three, the master curves and relaxation time spectra can be constructed to give the full picture of K' and K" over all frequencies at temperature from T_g to about 100 to 150°C above T_g. In Table 1 below provisional values of these parameters are given for three other samples that have been measured in detail by the high-precision method to date. While not final, they serve to indicate the ranges of values to be expected for these parameters.

It may be pointed out that the computed loss tangent K"/K' at x=0 implicit in Fig. 6 is given by $\Delta K/2K'$, as can be seen from Eqs. (19) and (20). An average value for the loss tangent thus computed from the data in Table 1 is close to 20%. In all the experiments reported here the loss tangent was always an order of magnitude smaller than this. This lends experimental support to the suggestion presented earlier that ΔK is not constant but dependent on frequency and temperature, in contrast to the main tenet of the WLF shift technique.

Table 1 - Provisional Values of Master Curve Parameters for Four Elastomers.

SAMPLE	K (GPa)	ΔK	α	T_{ref}
5109 Neoprene	2.23	1.1	0.037	27
5109S Neoprene	2.72	0.81	0.026	19
B252 Butyl	2.37	0.91	0.033	21
PR1526 Urethane	2.42	0.83	0.017	18

ACKNOWLEDGMENTS

The authors wish to acknowledge contributions of a number of NRL-USRD staff who assisted with this experimental program. Early work on bulk modulus measurements was done at NRL-USRD by M. C. Komelaski and reported in detail in a thesis [26]. Much valuable experimental assistance was given at various stages in the development of the present apparatus and procedure by Chris Colquit who prepared the transducers and wrote the computer program to operate the experiment; Elaine Browder, Cathy Ramzy, Jim Wilson, and Joe Morales collected much of the experimental data; Virgil Apostolico, with Joe Morales, completed and refined the second coupler system originally built by Chris Colquit.

REFERENCES

1. Capps, R.N., "Dynamic Young's moduli of some commercially available polyurethanes," J. Acoust. Soc. Am. 73, 2000 (1983).

2. Goldberg, H., and Sandvik, O., "Instrument for measuring rheological properties of elastic fluids," Analytical Chem. 19, 123 (1947).

3. Adkins, R.L., "Design considerations and analysis of a complex-modulus apparatus," Experimental Mechanics 6, 362 (1966).

4. Capps, R.N., "Influence of carbon black fillers on acoustic properties of polychloroprene (neoprene) elastomers," J. Acoust. Soc. Am. 78, 406 (1985).

5. McKinney, J.E., Edelman, S., and Marvin, R.S., "Apparatus for the direct determination of the dynamic bulk modulus," J. Appl. Phys. 27, 425 (1956).

6. Cohen, M.H., and Grest, G.S., "Liquid-glass transition, a free volume approach," Phys. Rev. B 20, 1077 (1979).

7. Cohen, M.H., and Turnbull, D., "Molecular transport in liquids and gases," J. Chem. Phys. 31, 1164 (1959).

8. Bueche, F., "Physical Properties of Polymers," (John Wiley & Sons, New York, 1962) (Reprinted by Robert Krieger Publishing Co., Pt. Malabar, FL, 1979), pp. 95-96.

9. Turnbull, D., and Cohen, M.H., "Free-volume model of the amorphous phase: glass transition," J. Chem. Phys. 34, 120 (1961).

10. Bueche, F., Ref. 8, p. 106.

11. Williams, M.L., Landel, R.F., and Ferry, J.D., "The temperature dependence of relaxation mechanisms in amorphous polymers and other glass-forming liquids," J. Am. Chem. Soc., 77, 3701 (1955).

12. Ferry, J.D., "Viscoelastic Properties of Polymers," 3rd Ed., (John Wiley & Sons, New York, 1980), pp. 267, 271, 275, and Ch. 11.

13. Ferry, J.D., Ibid, p. 276.

14. Perepechko, I.I., "An Introduction to Polymer Physics," English Translation (MIR Publishers, Moscow, 1981), Ch. 7.

15. Fuoss, R.M. and Kirkwood, J.G., "Electrical properties of solids. VIII. Dipole moments in polyvinyl chloride-diphenyl systems," J. Am. Chem. Soc. 63, 385 (1941).

16. Bueche, F., Ref. 8, pp. 166-167.

17. Ferry, J.D., Ref. 12, Ch. 10.

18. Doolittle, A.K., "Studies in Newtonian flow II. The dependence of the viscosity of liquids on free-space," J. Appl. Phys. 23, 418 (1952).

19. Ferry, J.D., Ref. 12, pp. 276-279.

20. McKinney, J.E., and Belcher, H.V., "Dynamic compressibility of poly(-vinyl acetate) and its relation to free volume," J. Res. NBS, 67A, 43 (1963).

21. Bueche, F., Ref. 8, p. 87.

22. Rouse, P.E., Jr., "A theory of the linear viscoelectric properties of dilute solutions of coiling polymers," J. Chem. Phys. 21, 1272 (1953).

23. Ferry, J.D., Ref. 12, pp. 344-349.

24. Bobber, R.J., "Underwater Electroacoustic Measurements," (U.S. Government Printing Office, Washington, DC, 1970), p. 40.

25. Timme, R.W., "Speed of sound in castor oil," J. Acoust. Soc. Am. 52, 989 (1972).

26. Komelaski, M.C., "A method for measuring the dynamic bulk modulus and loss factor in hydroacoustic materials," Master's Thesis, Florida Institute of Technology, Melbourne, FL, 1976.

BLANK PAGE

Appendix A

HOLE SIZE PROBABILITY DISTRIBUTION

The expression given by Eq. (1) for the probability p(q) that there will be exactly q packets of free volume each of size v_f associated with a given molecule in a solid with N molecules may be derived by the following argument.

Consider N boxes (corresponding to N molecules in a sample) to be filled at random by N balls (packets of size v_f). The chance that a given ball will go into a given box is 1/N, and the chance that it will not go into a given box is [1-(1/N)]. Therefore, the chance that a given box will end up with q balls is the chance $(1/N)^q$ that q balls will go into the box, multiplied by the chance $[1-(1/N)]^{(N-q)}$ that (N-q) balls will not go into the box.

There are N!/(N-q)!q! permutations of the N boxes with q balls in a box. Hence, the total probability for there to be exactly q packets of free-volume v_f associated with a given molecule is the product of the three independent probability factors above. Since N is very large, and much larger than q, it follows that $[1-(1/N)]^{(N-q)}$ is approximately $[1-(1/N)]^N$.

A fundamental definition for the base e of natural logarithms is

$$e^{-1} = \lim_{N\to\infty} [1-1/N]^N \tag{A1}$$

so the term $[1-(1/N)]^N$ becomes simply e^{-1}.

The permutation factor in the limit of large N becomes approximately

$$\frac{N!}{q!\,(N-q)!} = \frac{N(N-1)\,(N-2)\ldots\ldots(N-q+1)}{q!} = \frac{N^q}{q!} \tag{A2}$$

and p(q) becomes approximately $e^{-1}/q!$

Using Stirling's approximation for the factorial q! gives

$$p(q) \approx \frac{1}{\sqrt{2\pi q}} \exp\,[-q(\ln q-1) - 1]. \tag{A3}$$

Since $q=v_f'/v_f$ where v_f' is the actual amount of free volume associated with a molecule, the final probability that a molecule has free-volume v_f' associated with it is

$$p(v_f') = \sqrt{\frac{v_f}{2\pi v_f'}} \exp\ (-av_f'/v_f) \qquad \text{(A4)}$$

where $a=\ln(q)-1$ and the (-1) term in the exponential has been dropped since $q>>1$ in the present application.

Appendix B

FUOSS AND KIRKWOOD FORMULATION

The method of Fuoss and Kirkwood* can be shown in somewhat abbreviated form by starting from expressions for K' and K" for the simple case of a single relaxation time, τ. The equations are the same as Eqs. (14) and (15):

$$K' = K'_o + \Delta K \frac{(\omega\tau)^2}{1 + (\omega\tau)^2} \tag{B1}$$

$$K'' = \Delta K \frac{\omega\tau}{1 + (\omega\tau)^2} \tag{B2}$$

with the terms K'_o, and ΔK having the same meanings as before.

These equations may be generalized easily to the case of any number of relaxation times**

$$K' = K'_o + \Delta K \sum_{j=1} G_j \frac{(\omega\tau_j)^2}{1 + (\omega\tau_j)^2} \tag{B3}$$

$$K'' = \Delta K \sum_{j=1} \frac{\omega\tau_j}{1 + (\omega\tau_j)^2} \tag{B4}$$

where the new factors G_j are related in some way, as yet undetermined, to the distribution of relaxation times, τ. Since the G_j appears in both K' and K", if the problem can be treated more easily in K", as is the case, then the solution obtained for K" can be transformed for use in K'.

*Fuoss, R.M. and Kirkwood, J.G., "Electrical Properties of Solids. VIII. Dipole Moments in Polyvinyl Chloride-Diphenyl Systems," J. Am. Chem. Soc. 63, 385 (1941).

**Ferry, J.D., "Viscoelastic Properties of Polymers," 3rd Ed., (John Wiley & Sons, New York, 1980), p. 276.

Note that K" has the general form shown in Fig. B1 below.

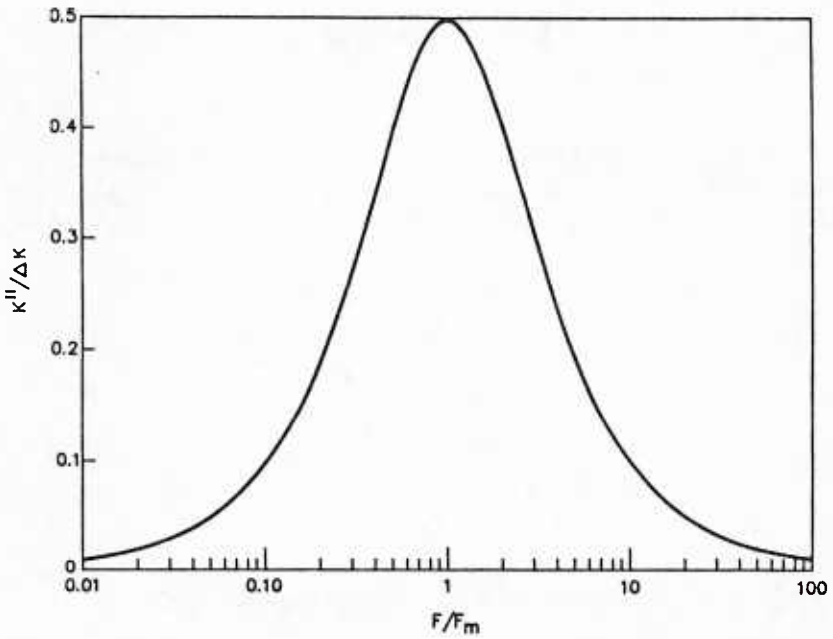

Fig. B1 - Loss modulus K" as a function of frequency for a single relaxation time. The abscissa is on a log scale where $x=\ell n(\omega/\omega_m)=\ell n(f/f_m)$.

The subscript m denotes the value at which K" has its maximum. The constraint that there be only one relaxation time also means that there will be only one maximum of K", or one inflection point of K'.

It is desirable at this point to normalize $(K^*-K'_o)$ by dividing by ΔK. Let a new, reduced, complex bulk modulus be defined by

$$Q(\omega) = \frac{K^* - K'_o}{\Delta K} = \sum_{j=1}^{n} \frac{i\omega\tau_j G_j}{1 + i\omega\tau_j} = J + iH \qquad \text{(B5)}$$

where $K^*=K'+iK"$.

Equation (B5) thus defines a reduced storage modulus, J, and a reduced loss modulus, H. For a continuous distribution of relaxation times with spectral density $G(\tau)$, $Q(\omega)$ should have the following general form, by extension of the corresponding form given by Perepechko*

*Perepechko, I.I., "An introduction to polymer physics," English Translation (MIR Publishers, Moscow, 1981), Ch 7.

$$Q(\omega) = \int_0^\infty \frac{i\omega\tau\, G(\tau)}{1 + i\omega\tau}\, d\tau = \int_0^\infty \frac{G(\tau)(\omega\tau)^2}{1 + (\omega\tau)^2}\, d\tau + i \int_0^\infty \frac{\omega\tau G(\tau)}{1 + (\omega\tau)^2}\, d\tau. \qquad \text{(B6)}$$

It remains for $G(\tau)$ to be identified with physical parameters such as K'_o, ΔK, etc. From Eqs. (B5) and (B6) it is evident that

$$J = \frac{K' - K'_o}{\Delta K} = \int_0^\infty \frac{G(\tau)(\omega\tau)^2}{1 + (\omega\tau)^2}\, d\tau \qquad \text{(B7)}$$

$$H = \frac{K''}{\Delta K} = \int_0^\infty \frac{G(\tau)\ \omega\tau}{1 + (\omega\tau)^2}\, . \qquad \text{(B8)}$$

The relaxation times τ may be normalized by a factor τ_m chosen to make $\omega_m\tau_m=1$ (assuming that $H(\omega)$ has a single maximum at $\omega=\omega_m$). Then new variables x and s may be introduced.

$$x = \ln(\omega/\omega_m) \quad \text{and} \quad s = -\ln(\tau/\tau_m)$$

so

$$\omega\tau = \exp\,(x-s). \qquad \text{(B9)}$$

Substituting the new variables into Eq. (B8) and noting that in the integrations ω and x are considered fixed so $ds=-d\tau/\tau$,

$$H(x) = \int_0^\infty \frac{-\tau G(\tau)\ \exp(x-s)}{1 + \exp[2(x-s)]}\, ds \qquad \text{(B10)}$$

Introduce a new function F(s) defined by

$$F(s) = -\tau G(\tau) = -\tau_m e^{-s} G\ (\tau_m e^{-s}) \qquad \text{(B11)}$$

Then

$$H(x) = \int_0^\infty \frac{F(s)\ \exp\ (x-s)}{1\ +\ \exp\ [2(x-s)]}\ ds = \int_0^\infty F(s)\ L(x-s)\ ds \qquad \text{(B12)}$$

where

$$L(x) = \frac{e^x}{1\ +\ \exp 2x} = \frac{1}{2}\ \text{sech}\ x\ . \qquad \text{(B13)}$$

Note that Eq. (B12) expresses H(x) in the form of a convolution of the functions F and L.

Taking Fourier transforms of both sides of Eq. (B12) yields

$$F_u(H) = \int_{-\infty}^{\infty} H(x)\exp(iux)\ dx = \int_{-\infty}^{\infty}\int_{-\infty}^{\infty} L(x-s)F(s)\exp(iux)\ dxds =$$

$$\int_{-\infty}^{\infty} L(t)\exp(iut)\ dt \int_{-\infty}^{\infty} F(s)\exp(ius)\ ds = F_u(L)\ F_u(F) \qquad \text{(B14)}$$

where $F_u(H)$ signifies the transform of the function H with transform variable, u. Solving for $F_u(F)$, the transform of F(s), and using the inversion theorem, one gets

$$F(s) = \frac{1}{2\pi}\int_{-\infty}^{\infty} F_u\ (F)\exp(-ius)\ du = \frac{1}{2\pi}\int_{-\infty}^{\infty} \frac{F_u(H)}{F_u(L)}\ \exp(-ius)\ du. \qquad \text{(B15)}$$

This equation can be simplified if a functional form can be found for the kernel, L. The proper form is given by Eq. (B13). Fuoss and Kirkwood have evaluated the Fourier transform of L by contour integration giving

$$F_u(L) = F_{-u}(L) = \frac{\pi}{2}\,\mathrm{sech}\left(\frac{\pi u}{2}\right) \tag{B16}$$

Therefore, Eq. (B15) may be written

$$F(s) = \frac{1}{\pi^2}\int_{-\infty}^{\infty}\cosh\left(\frac{\pi u}{2}\right)\,F_u(H)e^{-ius}\,ds \tag{B17}$$

$F_u(H)$ may be found experimentally by taking a Fourier transform of the reduced loss modulus $K''(\omega)/\Delta K$.

Alternatively, let $K''/\Delta K$ [$= H(x)$] be fitted by a function whose form we expect to be a suitably spread hyperbolic secant function of argument (αx) where α is the spread parameter. In logarithmic coordinates x write

$$H(x) = H(0)\ \mathrm{sech}(\alpha x) \tag{B18}$$

as the fitting function. The parameters $H(0)$ and α are to be determined from a best fit of this function to the experimental K'' data on a logarithmic frequency scale.

In the bulk modulus work, however, it is better to determine α by fitting the experimental $K'(x)$ curve rather than $K''(x)$, so it is necessary to see what the fitting function should be for K' corresponding with $\mathrm{sech}(\alpha x)$ for K''. Ordinarily this could be done most easily by using the Kramers-Kronig relations relating real and imaginary parts of a linear casual transform such as K^*.

In the present case, where $\alpha<1$, there are mathematical difficulties which complicate such a direct determination of K'. We therefore proceed along different lines. Going back to Eq. (B1) or (B3) for the case of a single relaxation time, we note that using logarithmic frequency coordinates, x, Eq. (B1) becomes, for the case $\alpha=1$,

$$K'(x) = K'_o + \frac{\Delta K}{2}\,[1 + \tanh(x)]\ . \tag{B19}$$

In a similar way, Eq. (B3) can be shown to give the Fuoss-Kirkwood result for K'' with $\alpha=1$, namely Eq. (B18) in the form

$$K''(x) = K''(0)\ \mathrm{sech}(x)\ . \tag{B20}$$

For the more general spread case this becomes

$$K''(x) = K''(0)\ \mathrm{sech}(\alpha x). \tag{B21}$$

We therefore take for the corresponding generalized $K'(x)$ the expression

$$K'(x) = K'_o + \frac{\Delta K}{2}\,[1 + \tanh(\alpha x)]. \tag{B22}$$

It should be noted that the slope of the $K'(x)$ curve given by Eq. (B22) at the center of the transition region where $x=0$ is simply $\alpha\Delta K/2$. This makes it easy to find the value of α from the experimental data fitted to the form of Eq. (B22) if the data covers the inflection region of K'.

The pair of expressions for K' and K'' in Eqs. (B21) and (B22) make it possible to find the loss modulus from the storage modulus K' which is more accurately found from experimental data than is K''. This provides a powerful way to obtain more accurate loss modulus values and is an important result of the dispersion relation approach to elastic moduli.

To determine the relaxation spectrum $G(\tau)$, one must first find $F(s)$ using Eq. (B17). This requires the Fourier transform $F_u(H)$ which can now be calculated explicitly from the expression for H in Eq. (B18). Fuoss and Kirkwood have done this, and the resulting expression for $G(\tau)$ is

$$G(\tau) = \frac{\alpha}{\pi}\frac{\tau_m}{\tau}\left[\frac{\cos\left(\frac{\alpha\pi}{2}\right)\cosh(\alpha s)}{\cos^2\left(\frac{\alpha\pi}{2}\right) + \sinh^2(\alpha s)}\right] \tag{B23}$$

where $s=-\ln(\tau/\tau_m)$ as usual.

Appendix C

DATA SMOOTHING PROCEDURES

The method used in this report to smooth the data and construct a master curve will be described in detail in this appendix since there are apparently some differences in procedure among various workers. We do not use the WLF method as described by Ferry* but employ what may be considered a variation of it making use of the linear form of the zero-frequency expression for K/T as set forth in Eq. (8), namely

$$[\ln(K/T)]^{-1} = d + bT. \tag{C1}$$

This equation permits the data at a given frequency but at several temperatures to be smoothed with respect to temperature by linear regression of $[\ln(K'/T)]^{-1}$ vs T. This procedure is carried out in the present work at two convenient frequencies, 0.1 and 1 kHz over a temperature range -10° to +40°C with data taken at 5°C intervals. Since K' is very nearly a linear function of frequency between 0.1 and 1 kHz over this temperature range, smoothing at the two frequencies with respect to temperature provides a series of short segments of K' vs frequency between 0.1 and 1 kHz, one for each temperature. These are plotted on a logarithmic frequency scale, one above the other, labeled by temperature. Then, beginning with the segment having the largest slope, each segment is shifted horizontally until it visually fits together with its neighbors forming a relatively smooth curve. This is similar to the procedure used in the regular WLF method to fit pieces of the K'(f) curve together. The fitting process is easier and better if the segments overlap considerably, and Ferry makes such overlap a condition for proper application of the WLF method. However, such overlap is not a rigid requirement when the following method is used.

Let Eq. (19) be written in three-parameter form:

$$K'(x) = A + B \tanh(\alpha x) \tag{C2}$$

where $A=(K'_o+K'_\infty)/2$, and $B=\Delta K/2$.

Then, using a parametric curve fitting routine, one finds the best values of the parameters A, B, and α the spread parameter. The result is a best fit to the function in Eq. (C2), best fit being determined by a least-squares criterion.

*Williams, M.L., Landel, R.F., and Ferry, J.D., "The temperature dependence of relaxation mechanisms in amorphous polymers and other glass-forming liquids," J. Am. Chem. Soc. 77, 3701 (1955).

An alternate approach is to perform a linear regression on each experimental K'(f) curve between 0.1 and 1 kHz. These linear segments of K' can then be plotted and shifted as described above, followed by the same parametric curve fitting. This procedure does not work as well. Apparently experimental variations in the slopes determined in this way are greater than when the smoothing with respect to temperature is done using Eq. (C1). For this reason, smoothing by means of Eq. (C1) has been used to obtain all the master curves reported here.

The theoretical slope of the K' curve obtained by differentiating Eq. (C2) is

$$dK'/dx = \alpha \frac{\Delta K}{2} \operatorname{sech}^2(\alpha x). \tag{C3}$$

A convenient frequency within the range of the experimental data is chosen, and experimental values of the slopes dK'/dx at this frequency are plotted against temperature. The resulting curve resembles Eq. (C3) since x is a function of temperature. The exact correspondence can be found by noting from the definitions of x [Eq. (16)] and the WLF shift factor, a_T, [Eq. (30)], that if the shift factor is referred to temperature T_m, at which the slope is a maximum or at which $x=x_m=0$ on the log frequency scale, we have the simple relation

$$x = -\ln(a_T) = \frac{c_1 (T-T_m)}{c_2 + (T-T_m)} . \tag{C4}$$

This equation makes it possible to translate Eq. (C3) from frequency to temperature as the independent variable, giving

$$dK'/dx = \alpha \frac{\Delta K}{2} \operatorname{sech}^2 \left[\frac{c_1 (T-T_m)}{c_2 + (T-T_m)}\right] \tag{C5}$$

where c_1 and c_2 are the WLF constants referred to temperature T_m.

Once the experimental slopes have been fitted to Eq. (C3) for the chosen frequency, smoothed values of the slopes can be used to improve the set of segments of K'(x), one for each temperature, which may then be used in the usual way to carry out the WLF shift process to obtain a master curve. In so doing, a reference temperature for the master curve must be chosen. It need not be T_m, and the choice is arbitrary, but it should lie somewhere within the experimental temperature range for best accuracy, as Ferry has pointed out.

The experimental master curve constructed as described above by the WLF method may then be fitted to Eqs. (19) or (24) to find the parameters K'_o, ΔK, and α which fully determine the shape of the master curve. Its position on the frequency scale; i.e., the value of f_m, is not determined by this fit, however.

Superintendent
Naval Postgraduate School
Attn: Technical Library
Monterey, CA 93943